LETTER TO THE EDITOR

Discovery of collimated ejection from the symbiotic binary BF Cygni[⋆]

A. Skopal[1], N. A. Tomov[2,⋆⋆], and M. T. Tomova[2]

[1] Astronomical Institute, Slovak Academy of Sciences, 059 60 Tatranská Lomnica, Slovakia
   e-mail: skopal@astro.sk
[2] Institute of Astronomy and NAO, Bulgarian Academy of Sciences, PO Box 136, 4700 Smolyan, Bulgaria

ABSTRACT

Context. Detection of collimated ejection from white dwarfs (WD) in symbiotic binaries is very rare and has employed a variety of methods in X-ray, radio, optical imagery, and spectroscopy. To date, its signature in the optical spectra has only been recorded for four objects (MWC 560, Hen 3-1341, StHα 190, and Z And).
Aims. We present the first observational evidence of highly-collimated bipolar ejection from the symbiotic binary BF Cyg, which developed during its current (2006-12) active phase, and determine their physical parameters.
Methods. We monitored the outburst with the optical high-resolution spectroscopy and multicolour $UBVR_CI_C$ photometry.
Results. During 2009, three years after the 2006-eruption of BF Cyg, satellite components to Hα and Hβ lines emerged in the spectrum. During 2012, they became stable and were located symmetrically with respect to the main emission core of the line. Spectral properties of these components suggest bipolar ejection collimated within an opening angle of $\lesssim 15°$, whose radiation is produced by an optically thin medium with the emission measure of $1-2 \times 10^{59} (d/3.8\,\mathrm{kpc})^2\,\mathrm{cm}^{-3}$.
Conclusions. Formation of the collimated ejection a few years after the eruption and its evolution on a time scale of years at a constant optical brightness can aid us in better understanding the accretion process during the active phases of symbiotic stars.

Key words. ISM: jets and outflows – binaries: symbiotic – stars: individual: BF Cygni

1. Introduction

BF Cyg is an eclipsing symbiotic binary (Skopal 1992; Pereira & Landaberry 1996) comprising an M5 III giant (Mürset & Schmid 1999) and a white dwarf (WD) on a 757.2-d orbit (e.g. Fekel et al. 2001). The historical light curve of BF Cyg is dominated by a symbiotic nova-like outburst, which occurred around 1895 (Jacchia 1941) with a slow decline to the pre-outburst magnitudes, for almost one century, and a number of Z And-type outbursts superposed on the nova-like profile (see Fig. 1 of Skopal et al. 1997; Leibowitz & Formiggini 2006; Siviero et al. 2012). During outbursts the emission line spectrum is represented by the lines of low ionized elements (H I, He I, and neutral or singly ionized metals), whose profiles are often P Cyg-type. Their absorption component indicates a mass outflow at $100-200$ to $500\,\mathrm{km\,s}^{-1}$ from the hot star (González-Riestra et al. 1990; Cassatella et al. 1992; Skopal et al. 1997; McKeever et al. 2011).

The recent outburst of BF Cyg started on 2006 July 31 (Munari et al. 2006), when the star's brightness increased from $U \sim 11.1$ to $U \sim 9.3$ during 2006 August (Skopal et al. 2007). The low ionization state of the emission line spectrum and development of P Cyg profiles of H I, He I, and some Fe II lines were reported by Sitko et al. (2006), Iijima (2006), and McKeever et al. (2011). An interesting feature of the current active phase is a high level of the star's brightness, which is kept

continuously at $U \lesssim 10$ from the 2006 eruption to the present, i.e. for >6.3 years (Skopal et al. 2012, Fig. 1 here).

Our spectroscopic monitoring of BF Cyg revealed for the first time the emergence of satellite-emission components to the Hα and Hβ emission lines from 2009. To date, similar emissions in the optical spectra of symbiotic stars have only been discovered for Hen 3-1341 (Tomov et al. 2000), StHα 190 (Munari et al. 2001), and Z And (Skopal & Pribulla 2006), although a few jets have been discovered by other methods. In this contribution we present the evolution of these jet features from their emergence in 2009 to 2012 and determine their basic parameters.

2. Observations and data reduction

Our spectroscopic observations were carried out at the David Dunlap Observatory, University of Toronto (DDO) and the Rozhen National Astronomical Observatory (RNAO). At the DDO the high-resolution spectroscopy was performed by the single dispersion slit spectrograph equipped with a Jobin Yovon Horiba CCD detector (2048×512 pixels of $13.5\,\mu$m size; thinned back illuminated chip) mounted at the Cassegrain focus of the 1.88-m telescope. The resolution power was 12 000 and 8000 around the Hα and He II 4686−Hβ regions, respectively. During each night two very different exposures were applied to obtain a well-defined Hα profile and the continuum.

At the RNAO the high-resolution spectroscopy was carried out by the single dispersion slit spectrograph equipped with the Photometrics CCD camera (1024×1024 pixels of $24\,\mu$m size) mounted at the coudé focus of the 2-m RCC telescope. The
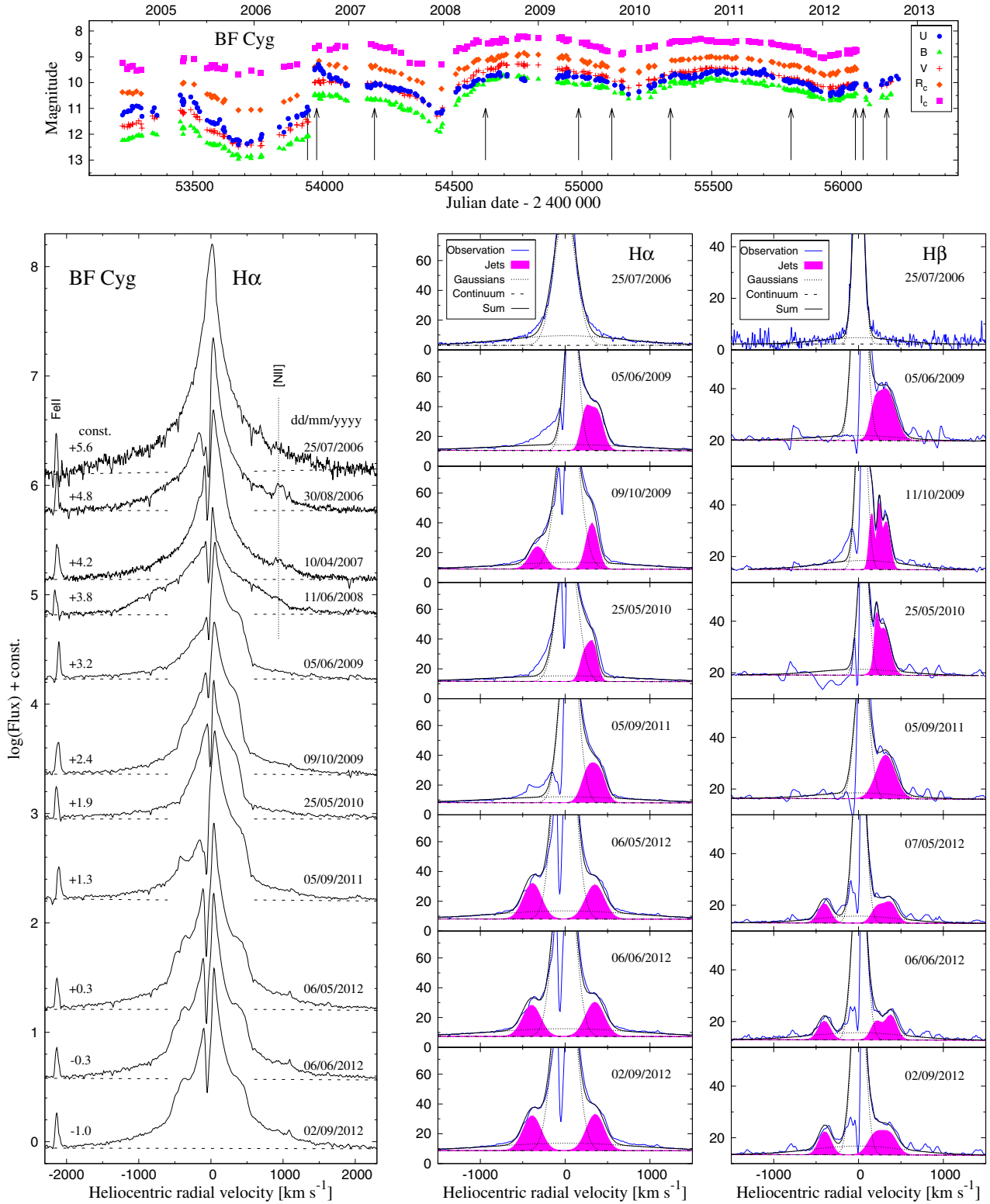

Fig. 1. *Top panel*: $UBVR_C I_C$ light curves of BF Cyg covering its current, 2006-12, active phase (Skopal et al. 2007, 2012, and our unpublished data for >2011.9). Arrows indicate times of our spectroscopic observations. *Lower panels*: evolution of the Hα and Hβ line profiles along the outburst. The filled curves represent the jet emission components (Sect. 3.2). Fluxes are in 10^{-13} erg cm^{-2} s^{-1} Å^{-1}.

resolution power was 32 000 and 24 000 around the Hα and Hβ regions, respectively. To obtain a better signal-to-noise ratio, two exposures per night were made in some cases.

Basic treatment of the spectra was done using the IRAF-package software. The spectra were converted to fluxes in erg cm^{-2} s^{-1} Å^{-1} with the aid of the (near-)simultaneous

$BVR_C I_C$ photometry corrected for emission lines. Uncertainties of such a continuum calibration are a few percent for the star's brightness around 9 mag in the VR passbands (see Skopal 2007, in detail). Observations were dereddened with $E_{B-V} = 0.35$ (Mürset et al. 1991). The journal of spectroscopic observations is given in Table 1.

Table 1. Log of spectroscopic observations.

Date dd/mm/yyyy	Julian date JD − 2 400 000	Region [nm]	T_{exp} [min]	Observatory
25/07/2006	53 941.843	642–671	10	DDO
	53 941.857	462–492	1+5	DDO
30/08/2006	53 977.621	642–671	2+10	DDO
	53 977.602	462–492	2+20	DDO
10/04/2007	54 200.860	642–671	1+15	DDO
	54 200.908	462–492	20	DDO
11/06/2008	54 628.828	642–671	2+30	DDO
	54 628.801	462–492	2+30	DDO
05/06/2009	54 988.461	649–670	20	RNAO
	54 988.496	478–498	20	RNAO
09/10/2009	55 114.289	649–670	15	RNAO
11/10/2009	55 116.248	478–498	20	RNAO
25/05/2010	55 342.420	647–667	20	RNAO
	55 342.467	478–498	2 × 20	RNAO
05/09/2011	55 810.300	647–667	20	RNAO
	55 810.318	478–498	20	RNAO
06/05/2012	56 054.470	647–667	20	RNAO
07/05/2012	56 054.517	478–498	2 × 20	RNAO
06/06/2012	56 085.461	647–667	20	RNAO
	56 085.480	478–498	20	RNAO
02/09/2012	56 173.276	642–662	20	RNAO
	56 173.254	473–493	20	RNAO

3. Results

3.1. Evolution in the Hα and Hβ lines

Figures 1 and 2 show evolution of the Hα and Hβ profiles from the 2006 brightening to 2012 September. The broad wings expanding to $\sim\pm2000$ in Hα and $\sim\pm1000\,\mathrm{km\,s^{-1}}$ in Hβ, were present in all spectra. Significant variations were observed mainly at/around the line cores. We summarize them as follows.

(i) Just prior to the main brightening in 2006 August (2006 July 25 spectrum), the profiles showed a single emission peak with the broad wings.

(ii) During the 2006 eruption, a sharp absorption developed on the blue side of the profile throughout the whole active phase. At some times, the Hβ profile was P Cyg type.

(iii) During 2009, additional satellite emission bumps appeared on the sides of the Hα and Hβ emission core, placed at a few times $100\,\mathrm{km\,s^{-1}}$ from the line center (Table 2).

(iv) During 2009–2011, the red satellite emissions were more pronounced, because of a strong absorption from the blue side of the line, which often consumed the blue Hβ wing totally. During 2010 May–2012 May, the blue Hβ satellite component transformed from absorption into emission.

(v) During 2012, the satellite emissions occurred on both sides of the Hα and Hβ lines, nearly symmetrically with respect to their central emission (the dotted line in Fig. 1).

3.2. Parameters of the satellite components

To isolate the satellite components from the whole line profile, we formally fitted the emission line core and its extended foot component with the Gaussian function (dotted lines in Fig. 1). We assumed them to be symmetrical with respect to the reference wavelength as suggested by observations during 2012 and before the eruption. Then the residual emissions were fitted with additional Gaussians (Fig. 1). From their parameters (the central wavelength, maximum I, and the width σ), we derived
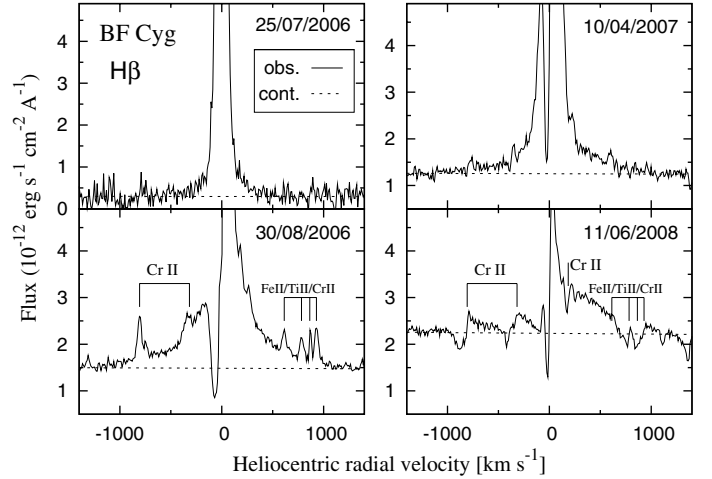

Fig. 2. Evolution in the Hβ line profile from around the 2006 August eruption to the formation of jets in 2009 (see Fig. 1), showing the pronounced absorption in P Cyg profiles of low-ionized metal lines at the spectrum from 11/06/2008, prior to detecting jets in 2009.

their radial velocity, RV_S, flux $F_S = \sqrt{2\pi}\,I\,\sigma$ and the width $FWHM_S = 2\sqrt{2\ln(2)}\,\sigma$. If more Gaussians were used to fit the satellite component, the above-mentioned parameters were estimated from their sum. Finally, we corrected the heliocentric radial velocity RV_S for the systemic velocity and the orbital motion of the hot component as given by elements of Fekel et al. (2001). Resulting parameters are introduced in Table 2. This approach and the resolution of our spectra allowed us to estimate uncertainties in the RV_S to $10-20\,\mathrm{km\,s^{-1}}$, in the $FWHM_S$ to 0.4 Å and in fluxes to 10–20% of the observed values.

The relatively small width of the satellite components ($FWHM_S = 245 \pm 11\,\mathrm{km\,s^{-1}}$; the average from all values in Table 2 and the rms error) and their position RV_S in the line profile suggest that these emissions are produced by radiation of a highly collimated ejection by the central star.

3.3. Opening angle of the jets

The narrow profile of satellite lines with often sharp edges and a flat top (see Fig. 1) allows us to assume a constant velocity of the emitting particles in the jet. Then the observed line width can be the result of the dispersion in the line-of-sight velocity components of the jet particles. This can be fulfilled if the jet emitting medium has the geometry of a narrow cone with the peak at the central object and it is characterized by a small opening angle θ_0. Assuming that the jets were launched perpendicularly to the disk plane that coincides with the orbital one, the opening angle can be expressed as a function of the observed width of the satellite component $HWZI_S$, RV_S and the orbital inclination i as

$$\theta_0 = 2\,\sin^{-1}\left[\frac{HWZI_S}{RV_S\tan(i)}\right], \qquad (1)$$

where $HWZI_S$ can be approximated with $FWHM_S$ (see Skopal et al. 2009, in detail). The orbital inclination is high, because of eclipses measured in both the optical and far-UV continuum (see Sect. 1). Skopal et al. (1997) estimated $i \approx 70°-90°$. For the purpose of this paper, we adopted $i = 80°$. Such a high i is consistent with the mass function of $0.0239\,M_\odot$, the mass ratio of ~3.8, and the considered mass of the WD, $M_{WD} = 0.6\,M_\odot$ (Fekel et al. 2001). Corresponding parameters from Table 2 yield the average value of $\theta_0 = 15°.2 \pm 1°.5 \times \Delta i$, where the uncertainty represents

Table 2. Parameters of Gaussian fits to the satellite emissions in Hα and Hβ lines.

Date dd/mm/yyyy	Line	RV_S S^-	S^+	$FWHM_S$ S^-	S^+	θ_0 S^-	S^+	F_S S^-	S^+	EM_{jet} S^-	S^+
05/06/2009	Hα	–	+298	–	270	–	18.4	–	18.0	–	17
	Hβ	–	+295	–	302	–	20.8	–	10.1	–	25
09/10/2009	Hα	–334	+308	215	161	13.0	10.6	7.5	11.7	7.1	11
11/10/2009	Hβ	–	+221	–	249	–	22.9	–	8.2	–	21
25/05/2010	Hα	–	+332	–	203	–	12.4	–	12.1	–	11
	Hβ	–	+291	–	192	–	13.4	–	6.9	–	17
05/09/2011	Hα	–	+317	–	274	–	17.5	–	16.7	–	16
	Hβ	–	+301	–	261	–	17.6	–	7.7	–	20
06/05/2012	Hα	–361	+375	248	258	13.9	13.9	13.8	13.8	13	13
07/05/2012	Hβ	–378	+334	167	302	8.9	18.3	2.2	4.0	5.6	10
06/06/2012	Hα	–368	+377	248	258	13.6	13.9	12.1	13.8	11	13
	Hβ	–376	+333	167	319	9.0	19.4	2.1	4.4	5.3	11
02/09/2012	Hα	–363	+381	247	247	13.8	13.1	13.5	14.1	13	13
	Hβ	–370	+307	214	344	11.7	22.7	2.6	5.5	6.6	14

Notes. Radial velocity RV_S [km s^{-1}], $FWHM_S$ [km s^{-1}], opening angle θ_0 [°], flux F_S [10^{-12} erg cm^{-2} s^{-1}], and emission measure EM_{jet} [10^{58} cm^{-3}].

a total differential of the function (1) for the uncertainty in the orbital inclination, Δi.

However, if the width of satellite components is in part caused by the velocity dispersion along the jet, then the opening angle will be $<\theta_0$.

3.4. Emission measure of the jets

Assuming that the radiation of jets is generated by the recombination transition in a line l (see Skopal et al. 2009), the luminosity $L_{jet}(l)$ is related to the line emissivity, $\varepsilon_l n_e n_p$ by

$$L_{jet}(l) = \varepsilon_l \int_{V_{jet}} n_e n_p \, \mathrm{d}V = \varepsilon_l \times EM_{jet}, \qquad (2)$$

where ε_l is the volume emission coefficient of the line transition, n_e and n_p are the concentrations of electrons and protons, V_{jet} and EM_{jet} are the volume and emission measures of the jets. Thus, neglecting dependencies of ε_l on the electron temperature and density means EM_{jet} can be expressed as

$$EM_{jet} = 4\pi d^2 \frac{F_S}{\varepsilon_l}. \qquad (3)$$

The last column of Table 2 introduces quantities of EM_{jet} for jet fluxes F_S, distance $d = 3.8$ kpc (Skopal 2005), and coefficients $\varepsilon_\alpha = 1.83$ for Hα and $\varepsilon_\beta = 0.682 \times 10^{-25}$ erg cm^3 s^{-1} for Hβ ($T_e = 2 \times 10^4$ K, e.g. Hummer & Storey 1987).

4. Conclusion

In this paper we reported a discovery of collimated ejection from the symbiotic star BF Cyg. The jets were indicated in the spectrum as satellite emission components to Hα and Hβ lines, which developed from 2009 – three years after the optical eruption. During 2012, they became bipolar (see Fig. 1). Parameters of satellite components suggest that the jets were collimated into the opening angle of $\lesssim 15°$, and their radiation was produced by an optically thin medium with the emission measure of $\sim 1-2 \times 10^{59}$ $(d/3.8$ kpc$)^2$ cm^{-3} (Table 2).

A detailed analysis of the present, unusually long-lasting outburst should aid us in better understanding the accretion process during active phases of symbiotic stars leading to formation of collimated ejection from their WDs.

References

Cassatella, A., Fernandez-Castro, T., Gonzalez-Riestra, R., & Fuensalida, J. J. 1992, A&A, 258, 368
Fekel, F. C., Hinkle, K. H., Joyce, R. R., & Skrutskie, M. 2001, AJ, 121, 2219
González-Riestra, R., Cassatella, A., & Fernández-Castro, T. 1990, A&A, 237, 385
Hummer, D. G., & Storey, P. J. 1987, MNRAS, 224, 801
Leibowitz, E. M., & Formiggini, L. 2006, MNRAS, 366, 675
Iijima, T. 2006, CBET, 633
Jacchia, L. 1941, Bull. Harv. Coll. Obs., 915, 17
McKeever, J., Lutz, J., Wallerstein, G., Munari, U., & Siviero, A. 2011, PASP, 123, 1062
Munari, U., Tomov, T., Yudin, B. F., et al. 2001, A&A, 369, L1
Munari, U., Siviero, A., Moretti, S., et al. 2006, CBET, 596
Mürset, U., & Schmid, H. M. 1999, A&AS, 137, 473
Mürset, U., Nussbaumer, H., Schmid, H. M., & Vogel, M. 1991, A&A, 248, 458
Pereira, C. B., & Landaberry, S. J. C. 1996, AJ, 111, 1329
Sitko, M. L., Lynch, D. K., Russell, R. W., & Venturini, C. C. 2006, IAUC, 8746
Siviero, A., Tamajo, E., Lutz, J., Wallerstein, G., & ANS Collaboration 2012, Baltic Astron., 21, 188
Skopal, A. 1992, IBVS, 3780
Skopal, A. 2005, A&A, 440, 995
Skopal, A. 2007, New Astron., 12, 597
Skopal, A., & Pribulla, T. 2006, ATel, 882
Skopal, A., Vittone A. A., Errico, L., et al. 1997, MNRAS, 292, 703
Skopal, A., Vaňko, M., Pribulla, T., et al. 2007, Astron. Nachr., 328, 909
Skopal, A., Pribulla, T., Budaj J., et al. 2009, ApJ, 690, 1222
Skopal, A., Shugarov, S., Vaňko, M., et al. 2012, Astron. Nachr., 333, 242
Tomov, T., Munari, U., & Marrese, P. M. 2000, A&A, 354, L25